Micromachining for Terahertz Applications

Victor M. Lubecke, *Associate Member, IEEE,* Koji Mizuno, *Fellow, IEEE,* and Gabriel M. Rebeiz, *Fellow, IEEE*

(Invited Paper)

***Abstract*— An overview of recent progress in the research and development of micromachined antennas, transmission lines, waveguides structures, and planar movable components for terahertz frequencies is presented. Micromachining is shown to provide a low-cost alternative to conventional (and very expensive) machined-waveguide technology, resulting in antennas with excellent radiation patterns, low-loss tuners, and three-dimensional (3-D) micromachined structures suitable for terahertz applications. Fabrication procedures for a variety of micromachined waveguide and planar structures are described here, along with measured terahertz performance. Applications of micromachining techniques for terahertz systems include focal-plane imaging arrays requiring a large number of elements and low-cost receivers for commercial and industrial applications such as pollution monitoring.**

***Index Terms*—MEMS, micromachining, millimeter wave, submillimeter wave, terahertz.**

I. Introduction

THE submillimeter-wave frequency range is usually defined from 300 GHz to 3 THz, corresponding to wavelengths between 1 mm and 100 μm. Recently, this frequency range has been included in the terahertz spectrum, which roughly extends from 100 GHz (3 mm) to 3 THz (100 μm). The primary application for terahertz technology has so far been terrestrial and astronomical remote sensing, where low-noise receivers are used to observe electromagnetic emissions resulting from physical and chemical processes in the atmosphere and outer space. Some key molecules like the hydroxyl radical (OH), which plays a critical role in all stages of ozone destruction and serves to remove harmful gases from the atmosphere, have significant emissions only at terahertz frequencies [1], [2]. Other applications for terahertz technology involve imaging systems demonstrated at around 94 GHz, which can be used to penetrate zero-visibility weather conditions (opaque even to infrared imaging systems) for aircraft guidance and landing or to identify plastic guns and explosives in noninvasive security and contraband detection systems [3]. These applications require sensitive receivers, particularly in the form of focal-plane imaging arrays, which can cover large detection areas with minimum scanning and integration times.

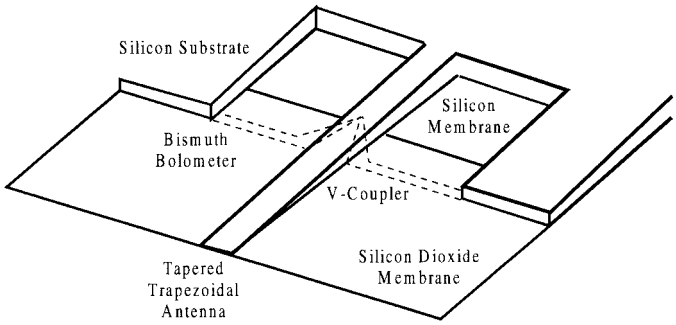

Fig. 1. 2.5-THz silicon dielectric-waveguide antenna with a membrane-supported bismuth bolometer load. A pioneering effort employed silicon micromachining to produce a 400-μm-long (3.5λ) by 40-μm-wide tapered-rod antenna with a well-defined directional beam [4].

As the desired wavelengths of operation become increasingly small, so do the dimensions for two-dimensional (2-D) and three-dimensional (3-D) antennas, quasi-optical lenses and mirrors, transmission lines, and related components. This makes terahertz technology well suited to high-resolution focal-plane imaging applications requiring large numbers of elements, and practical-size receiver systems for scientific, commercial, and industrial applications. Unfortunately, small dimensions make terahertz waveguide components difficult and costly to fabricate through conventional machining and assembly. Integrated-circuit technology offers practical advantages for terahertz systems, but planar components are subject to deleterious substrate modes and other loss mechanisms, which severely limit performance with increasing frequency of operation. Mechanical limitations imposed by waveguide dimensions and electronic limitations due to device parasitics also make it difficult to implement adjustable tuning and performance optimization in terahertz circuits.

Fortunately, novel applications of various micromachining techniques, which provide precise control of 2-D and 3-D structures at the 1–100-μm level, are demonstrating a practical means for producing a variety of high-performance terahertz front-end components. The application of micromachining technology to terahertz circuits was explored as early as 1979 [4], with the fabrication of a 2.5-THz 40-μm-wide by 400-μm-long (3.5λ) tapered-dielectric-rod antenna micromachined from a silicon substrate (see Fig. 1). Micromachining

Manuscript received March 20, 1998; revised August 11, 1998.

V. M. Lubecke is with the Photodynamics Research Center, The Institute of Physical and Chemical Research (RIKEN), Sendai 980, Japan (e-mail: victor@postman.riken.go.jp).

K. Mizuno is with the Photodynamics Research Center, The Institute of Physical and Chemical Research (RIKEN), Sendai 980, Japan, and is also with the Research Institute of Electrical Communication, Tohoku University, Sendai 980-77, Japan (e-mail: koji@riec.tohoku.acjp).

G. M. Rebeiz is with the Engineering and Computer Science Department, Radiation Laboratory, University of Michigan at Ann Arbor, Ann Arbor, MI 48109-2122 USA (e-mail: rebeiz@eecs.umich.edu).

Publisher Item Identifier S 0018-9480(98)08328-8.

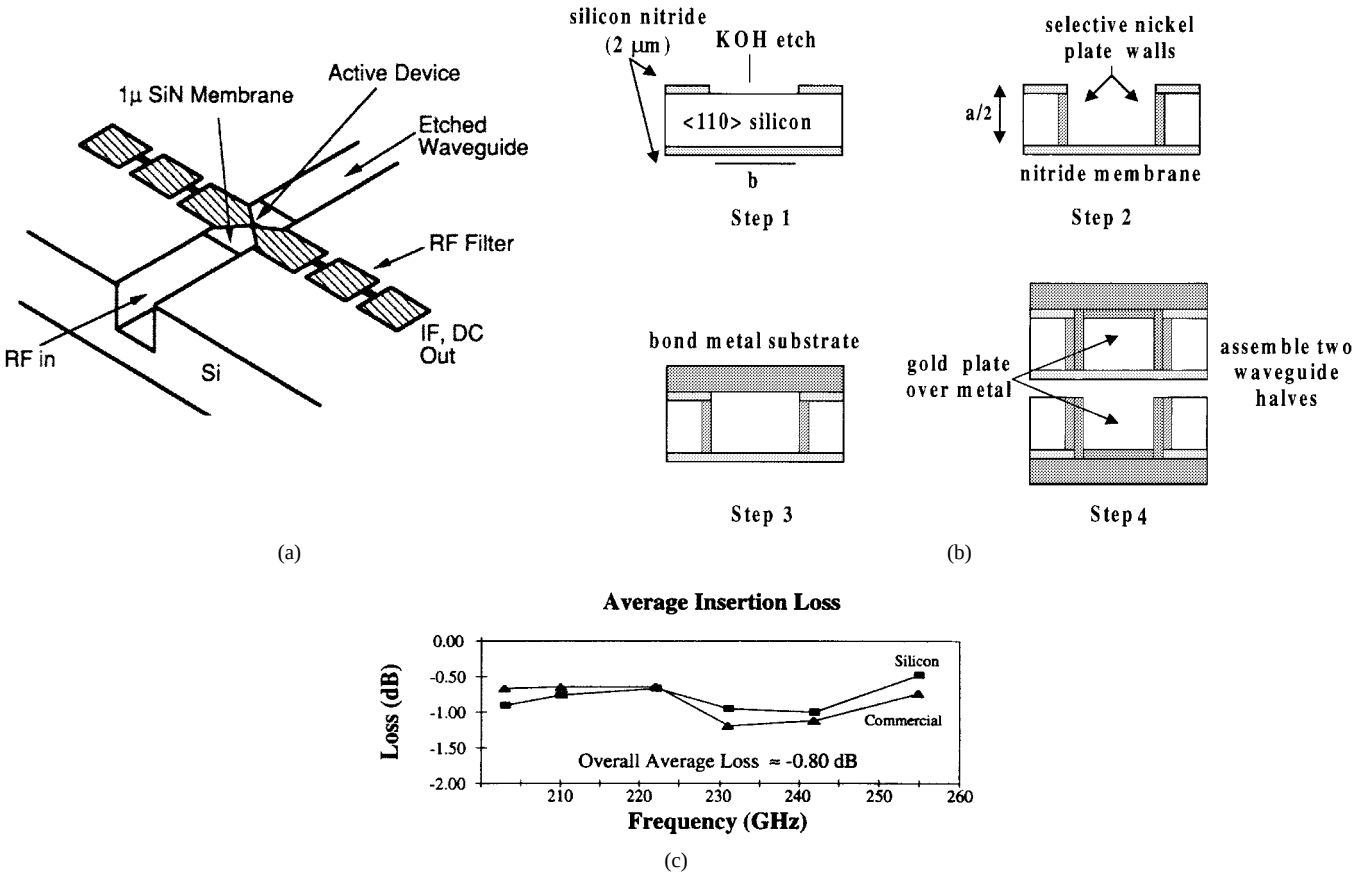

Fig. 2. (a) Concept, (b) fabrication overview, and (c) measured performance of silicon micromachined waveguides. Photolithography, anisotropic etching, and electro/electroless plating have been used to batch process split-waveguide halves with integrated membranes (accessible for device integration), with measured insertion loss S_{21} for the assembled waveguides (WR-4: $a = 1092\,\mu$m, $b = 546\,\mu$m) comparable to that of conventionally produced commercial waveguide [6].

technology not only allows for the extension of antennas and receiver front-end components to higher frequencies, but also allows higher levels of circuit integration and the realization of complicated networks and arrays. With the use of micromachining, it is possible to build a large number of terahertz receivers/subsystems for imaging-array applications at a relatively low cost, which is a major advantage over conventionally fabricated waveguide-based receivers.

This paper reviews various micromachining techniques used to produce high-performance terahertz circuits. Since front-end components are the most expensive and least reproducible components in a terahertz system, micromachining research efforts have concentrated on the development of miniature high-efficiency antennas, low-loss transmission-lines, and adjustable tuning structures. Terahertz micromachining technology can be broadly divided into three categories:

1) fabrication techniques which facilitate the frequency scaling of 3-D components from established waveguide designs;
2) techniques for suppressing substrate mode losses in planar integrated circuits by removing part or all of the dielectric around critical electromagnetic components;
3) techniques for integrating adjustable micromechanical components for low-loss circuit tuning and optimization.

These approaches are covered in detail in the following sections.

II. Frequency-Scaled 3-D Components

There are several examples of the application of micromachining technology to directly reproduce conventional 3-D waveguide and antenna components for terahertz frequencies. Micromachining research has been directed at fabricating such structures through photolithography, laser milling, and mold replication to allow the scaling of these designs to higher frequencies, fabrication of arrays and other intricate systems, and economical mass production. Waveguides micromachined from silicon and a mixer block produced from a mold have demonstrated performance equal to that of conventionally machined components at 255 and 690 GHz, respectively. This section describes the various micromachining techniques used for such components and discusses the measured results.

A. Silicon Waveguides

Micromachined waveguides can be economically batch processed from common silicon wafers, with critical dimensions determined through photolithography, anisotropic etching, and wafer thickness. Such waveguides are well suited to scaling for use at higher frequencies, and also include internal membrane structures on which thin-film devices could be readily integrated [5], [6]. This concept is illustrated in Fig. 2(a).

The process for fabricating miniature WR-4 ($a = 1092\,\mu$m, $b = 546\,\mu$m) silicon waveguides is shown in Fig. 2(b). A

thick 2-μm layer of silicon nitride (Si_3N_4) is first applied to each side of a double-side-polished 546-μm-thick silicon wafer with $\langle 110 \rangle$ surface orientation, through low-pressure chemical vapor deposition (LPCVD). The wafer thickness establishes one-half of the total width of the WR-4 waveguide (one-half of dimension a). Long rectangles are then defined on the backside of the wafer, through which openings are etched through the silicon nitride. The patterned silicon–nitride layer acts as an etch mask, and potassium hydroxide (KOH) is used to anisotropically etch straight-walled channels completely through the silicon wafer [7]. Accurate alignment of the channel masks to the $\langle 111 \rangle$ crystal plane of the silicon wafer is required to produce the extremely smooth sidewalls needed for minimizing high-frequency losses. The width of the channel defines the height of the WR-4 waveguide (dimension b). Selective electroless nickel deposition is used to provide a thin base layer of metallization to the silicon walls of the waveguide structure, and the wafer is bonded to a metal carrier using photoresist. An additional 3-μm layer of gold is electroplated over the conducting surfaces to enhance performance. The silicon–nitride membrane can then be patterned to support planar devices and tuning circuits before assembly with the top part of the waveguide (an identical structure with the silicon–nitride membrane removed). The plane where the two waveguide halves meet is noncritical since no RF currents are present at this interface in fundamental-mode operation. A similar process has been used to fabricate WR-10 ($a = 2540\,\mu$m, $b = 1270\,\mu$m) waveguides.

Silicon-etched waveguides were mounted in conventionally machined brass fixtures to allow connection to a standard-waveguide test system. Insertion-loss measurements S_{21} for 25.4-mm sections of both WR-10 and WR-4 waveguides were made from 75 to 110 and 200 to 255 GHz, respectively. The average measured loss was about 0.04 dB per wavelength for the WR-10 guide, and 0.80 dB per wavelength for the WR-4 guides. The WR-4 results are shown in Fig. 2(c). Both results are comparable to that of commercially available conventionally fabricated metal waveguides. While the fabrication of waveguides which include membranes has been demonstrated, devices have not yet been integrated.

B. Metal-Film Waveguides and Antennas

An alternative approach for micromachined waveguide fabrication has been demonstrated using photoresist as a form structure to produce thin-film metal guides with integrated horn antennas at either end. A simple arrangement of back-to-back slotted horn antennas with a length of waveguide between them, shown in Fig. 3(a), has been fabricated, with performance demonstrated at 200 GHz [8].

The process for fabricating this structure is as follows. A thick 100-μm layer of photoresist is spun onto a metalized substrate and photo patterned to produce a form structure for the waveguide and horn antennas. The width of the demonstrated waveguide was 1300 μm, and the flared antenna was 3965-μm-long and 5100-μm-wide at the maximum aperture. The form structure is covered by a thin layer of evaporated gold, followed by a thicker and, thus, stronger electroplated

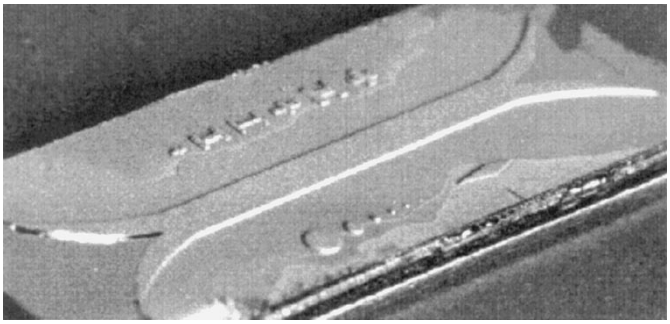

(a)

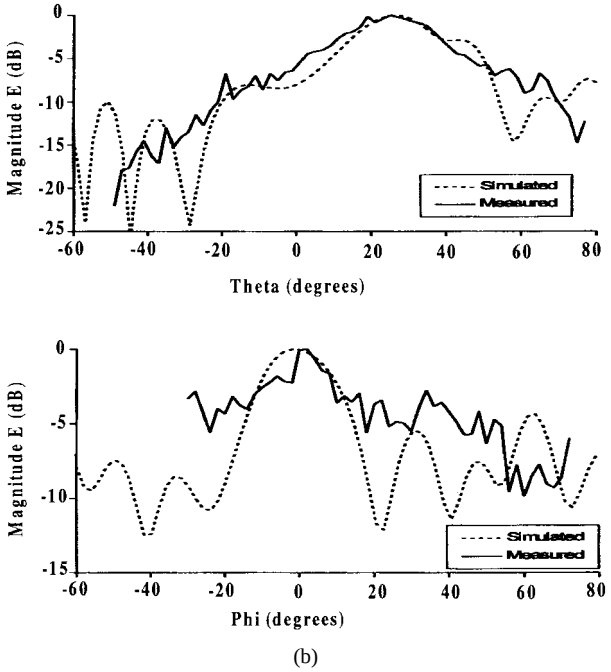

(b)

Fig. 3. (a) Photograph and (b) radiation patterns for a circuit consisting of a metal-film waveguide with integrated flared-horn antennas, fabricated through photoresist-forming techniques. The closed 1/8-height 200-GHz waveguide has cross-section dimensions of 80 μm $\times$ 1300 μm, and measured vertical plane (Theta) and horizontal plane (at 27°) (Phi) radiation patterns agree with theory [8].

layer of gold. A layer of thin photoresist is sprayed over the structure and patterned to allow etching of gold from the front of each slotted horn antenna. The resist is then stripped in acetone, leaving an air-filled guide with flared antenna openings at either end.

Antenna patterns for the circuit, shown in Fig. 3(b), were both simulated and measured at 200 GHz with good agreement. The beam radiated from the slotted horns at an angle of approximately 27° upwards from the horizontal plane of the substrate, with a 3-dB beamwidth of 31° in the vertical plane, and 23° in the horizontal plane. Guide losses and antenna efficiency have not yet been reported. While resist thickness limits the structure to a height which corresponds to about 1/8-height waveguide at 200 GHz, full-height waveguide could be implemented by scaling the design to higher frequencies (800 GHz). However, increasing the versatility of circuits made through this process requires the implementation of devices or other circuitry within the closed waveguide

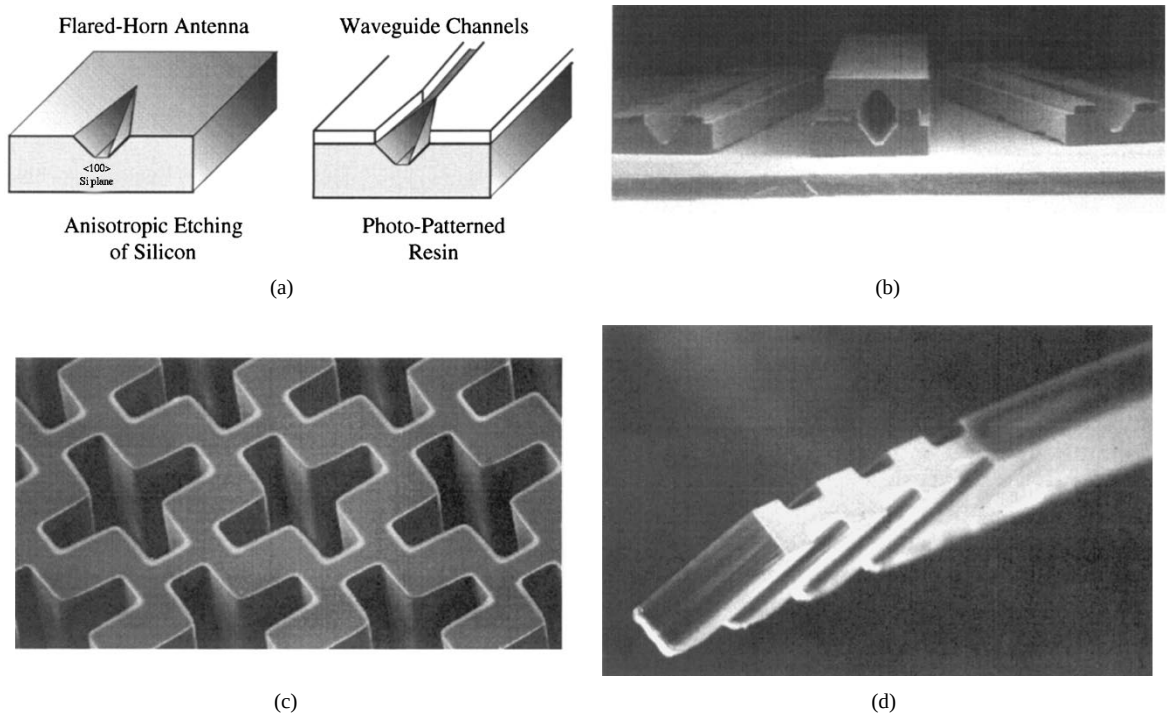

Fig. 4. (a) Concept and (b) SEM photograph of a mixer block designed for 585 GHz fabricated through silicon and thick photosensitive resin micromachining techniques [10], [11]. (c) SEM photographs of a high aspect-ratio dual-polarization dichroic plate for 640 GHz. (d) Noncontacting waveguide backshort for 2.5 THz, also fabricated with thick photosensitive resin [13], [14]. The waveguide channels in the mixer block are 200 μm $\times$ 400 μm, the crossed vertical-walled rectangular apertures for the 500-μm-thick dichroic plate are each about 400 μm $\times$ 100 μm and the tip of the backshort has dimensions of about 30 μm $\times$ 90 μm.

structure, which will require the development of additional technology [9].

C. Resin Waveguides with Silicon Antennas

Another method proposed for micromachined waveguides with integrated horn antennas combines both selective silicon etching and photosensitive resin techniques [10], [11]. Silicon micromachining is used to form a pyramidal horn antenna, which gradually tapers in a broad-band transition to join a waveguide made from photo-patterned resin, as illustrated in Fig. 4(a). Such technology can be used not only to fabricate mixer blocks and receiver arrays, but for other terahertz waveguide-based circuits like multipliers and bandpass filters as well. However, hybrid assembly of thin quartz substrates containing diodes, intermediate frequency (IF) filters, and dc bias circuitry is still required since the photosensitive resin is not readily compatible with existing membrane technology.

The fabrication technique has been demonstrated to produce a mixer block, shown in Fig. 4(b), on a scale suitable for 585-GHz operation. First, a mask with a shallow flare angle is aligned to the crystal orientation of a silicon wafer, allowing a V-type groove to be etched with sidewalls inclined at an angle of 54.7° to the wafer surface. A silicon dioxide (SiO_2) mask layer is used to define the pattern, and the etch is timed to yield a flat $\langle 100 \rangle$ surface at the bottom of the groove, resulting in the formation of one-half of the desired pyramidal horn. The wafer surface is then coated with a very thick 200-μm planarized layer of photosensitive resin (Epon SW-8 or similar) [12], which is subsequently photopatterned to form the vertical sidewalls of the adjoining waveguides. An additional layer of resin is used to form alignment pins to facilitate the assembly of the split-block design. The remaining resin is then heat-cured and the entire wafer is metalized through sputtering and electroplating. The split design provides access for the hybrid installation of devices and associated embedding circuitry, and formation of the waveguides and horns is completed when two halves are combined. While electrical performance has not yet been demonstrated, simulations using HP-HFSS indicate that the pattern of the pyramidal horn antenna can be tailored by simple variations in the fabrication process.

The practical high aspect-ratio characteristics of the photosensitive resin used in this example have also been applied for the formation of other terahertz components. Dichroic plates with perforations of complex shape and 10- or 100-μm scale features too small for conventional machining have been fabricated using similar resin. Enhanced resolution and uniformity have been obtained using a substrate-based mask and applied to create the 4-cm-diameter 500-μm-thick dual-polarization dichroic plate, with 100-μm scale holes designed to pass 640 GHz while blocking 240 GHz, shown in Fig. 4(c). Designs for other dichroic plates for use up to 1 THz have also been realized, and similar techniques have been employed to batch produce noncontacting waveguide backshorts for frequencies up to 2.5 THz, as shown in Fig. 4(d) [13], [14].

D. Alternative Techniques: Laser Micromachining and Resin Molding

In addition to the photolithographic techniques described, alternative machining techniques are also being developed

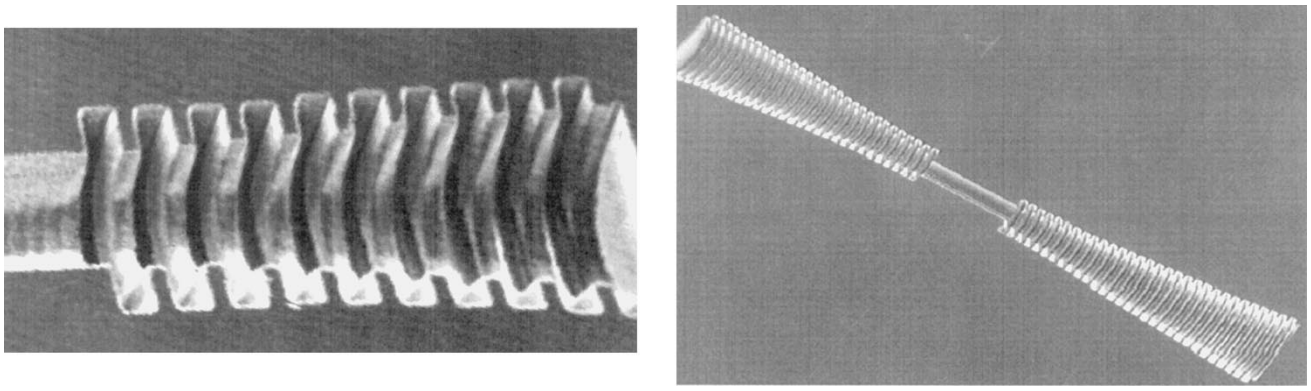

(a) (b)

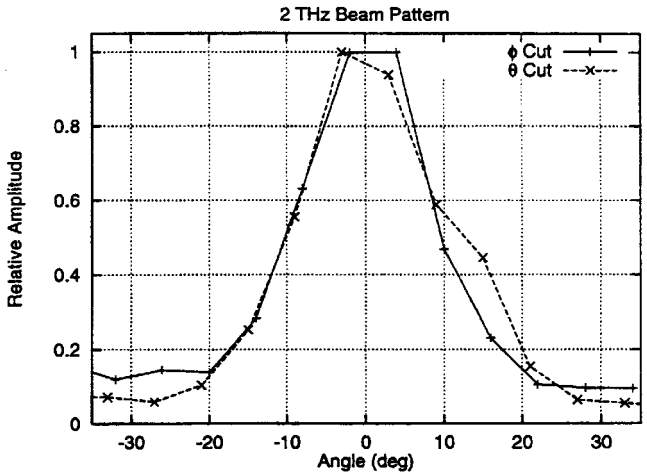

(c)

Fig. 5. (a) SEM photographs of a 2-THz corrugated feed horn milled from silicon with a laser. (b) Back-to-back feed horns replicated with a mold process, and measured radiation patterns for the latter. A 3-μm laser spot size was used to mill the original terahertz structure, and measured orthogonal radiation patterns ϕ and θ for the mold-produced structure are Gaussian [15].

for the fabrication of small-scale versions of conventional components.

1) Laser Micromachining: Computer-controlled laser milling of silicon has been used to fabricate corrugated feed horns and other components suitable for submillimeter-wave operation [15]. Unlike photolithographic micromachining, laser milling offers the advantage of unrestricted feature formation in the third dimension. It also allows for the fabrication of smaller features with improved tolerance over conventional milling without mechanically induced material damage. The process consists of the use of an argon–ion laser to locally heat a portion of a silicon substrate in a chlorine ambient environment. The molten silicon reacts with the chlorine to form volatile silicon chlorides, which are removed to form the desired features in the substrate.

The process has been used to produce corrugated feed-horn antennas, suitable for 810-GHz and 2.0-THz operation. The antennas were made by etching one-half of the structure in a substrate, and then assembling two halves to complete the structure. For the 810-GHz component, a laser spot size of 6 μm was used to produce 8-μm features, maintaining a shaving depth of approximately 1 μm and a rate of 10^5 μm^3/s. For the 2.5-THz component, shown in Fig. 5(a), a laser spot size of 3 μm was used to produce 4-μm features, maintaining a shaving depth of 0.65 μm and a rate of 5 $\times 10^4$ μm^3/s.

Additionally, a replication process was developed which allows multiple copies to be molded from a laser-milled master. After fluoridating the milled surface of the master, it is filled with polydimethylsiloxane (PDMS) to from a mold. A low-viscosity polymer precursor is then flowed over the mold and cured to form the copy and the mold is recovered to be used for further copies. The copy is sputter-coated with 0.3 μm of gold, and the two halves assembled using UV-curable epoxy. Nearly Gaussian antenna patterns were measured for a back-to-back feed-horn component, shown in Fig. 5(c) and (d), at 2 THz.

2) Resin Molding: A separate effort has been made to develop inexpensive high-precision copies of conventionally fabricated terahertz structures through the casting of polyurethane structures with a silicone-based mold formed from a master structure. The technique, illustrated in Fig. 6, is referred to as mastering, molding, and casting [11]. In this process, a silicone mold is formed on a conventionally machined master and then filled with polyurethane, which is subsequently cured and removed. The polyurethane components are then coated with sputtered gold, and an additional few micrometers of gold are added through electroplating. This effort has produced an

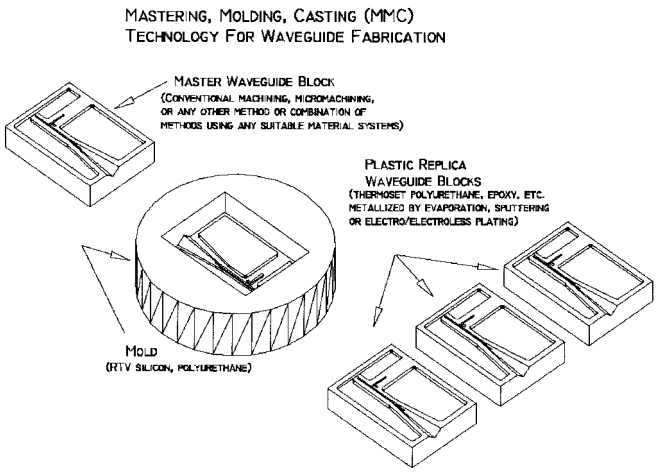

Fig. 6. Molding and casting technique used to replicate inexpensive copies of a terahertz component from a master [11]. Smooth waveguide features on the order of hundreds of micrometers have been accurately reproduced, and measured performance for a mold produced mixer block at 690 GHz are the same as that for a conventionally machined version.

entire mixer block, and measurements at 690 GHz have shown that the copies work as well as machined metal versions of the same design [16].

III. Membrane-Based Micromachined Components

An alternative to direct submillimeter-wave scaling of 3-D waveguide structures is the development of equivalent 2-D integrated-circuit structures. The performance of integrated-circuit antennas and transmission lines on high-dielectric constant substrates is severely limited by power radiation into substrate modes, an effect which increases as a function of both f^3 and $(\varepsilon_r, -1)^2$, where ε_r is the relative dielectric constant for the substrate [17]. Planar components are also subject to dielectric losses, which increase with frequency and can be prohibitively high for terahertz applications. One way to solve these problems is to integrate the antennas and transmission lines on very thin dielectric membranes (effectively making $\varepsilon_r = 1$). The membranes can be made very thin compared to a free-space wavelength, so that the antennas effectively radiate in free space. This technique eliminates dielectric- and substrate-mode losses, and the design can be easily scaled to different frequencies.

The fabrication of membrane-based components proceeds as follows: a 1–1.4-μm-thick three-layer structure of $SiO_2/Si_3N_4/SiO_2$ is deposited on a high-resistivity silicon substrate using thermal oxidation and LPCVD techniques. The layer must be in tension, resulting in flat and rigid membranes. The planar components (antennas, transmission lines, etc.) are patterned using standard photolithography. Next, an opening is defined on the backside of the wafer, underneath specific components through the use of an infrared aligner, and the silicon substrate is etched until the transparent dielectric membrane appears. The etchant used with silicon wafers is potassium hydroxide (KOH) or ethylene diamine pyrocatechol (EDP) [7], and both solutions result in a very low undercut rate and smooth sidewalls. The sidewalls form an angle of 54.7° with the planar top/bottom surfaces when a $\langle 100 \rangle$ silicon wafer is used. Via holes, if needed, are etched at the same time as the membranes are formed, and are electroplated with gold.

A. Integrated Horn Antennas and Imaging Arrays

Perhaps the most intricate membrane-type antenna is the integrated horn antenna. In this design, a dipole probe is suspended on a dielectric membrane in a pyramidal cavity etched in silicon [18]. The horn collects incident energy and focuses it to the probe antenna on the membrane. A Schottky-diode or a planar superconductor–insulator–superconductor (SIS) detector is typically integrated at the apex of the dipole, and the signal is taken out with a simple low-pass filter. The integrated horn array is composed of two or more stacked silicon wafers with a $\langle 100 \rangle$ crystal orientation. The horn cavity is made by anisotropic etching of the silicon wafers, which produces a horn flare-angle of 70.6°. The opening of the front wafer determines the horn aperture size, 1.5λ, while the thickness of the front wafer(s) determines the position of the dipole antenna inside the horn (0.38λ from the apex of the horn). The wafer stack (front and back wafers) is aligned and assembled together to form the integrated horn cavity, and the horn walls are coated with gold to reduce RF losses. An advantage of this approach is that the dipole/detector structures occupy an area which is much smaller than a unit cell in an array, leaving space for additional RF, IF, and dc electronics. A 16×16 element "CCD-like" imaging array with 1.4λ apertures has been demonstrated at 802 GHz [19]. At this frequency, the array period is 500 μm, yielding total array dimensions of 8×8 mm. The directivity of each antenna is 12 dB, which matches well with $f/0.75$ imaging system.

Integrated horn antennas can be designed to result in high antenna gains (up to 25 dB with metallic extensions) and very high Gaussian coupling efficiencies (more than 97%) (see Fig. 7). Schottky-diode heterodyne receivers based on this antenna have all resulted in state-of-the-art antenna patterns and receiver double sideband (DSB) performances (5.5-dB DSB at 94 GHz, 7.2 dB at 250 GHz, and 8.4 dB at 350 GHz), with practical 15%–20% bandwidths [20]–[23]. In this case, the planar Schottky diodes were placed at the apex of the dipole on the Si_3N_4 membrane using hybrid techniques, and silver epoxy was used to establish an electrical contact between the integrated dipole antenna and the Schottky diode. This arrangement has been tested by NASA, Jet Propulsion Laboratory, Pasadena, CA, and by Aerojet Corporation, Azusa, CA, and survived satellite-launch temperature and vibration tests. Recently, a 3×3 imaging array of micromachined horn antennas with thin-film SIS detectors and integrated tuning elements on silicon–nitride membranes was demonstrated with excellent antenna patterns and receiver DSB performance (30 K at 106 GHz and 50 K at 190 GHz, with the receiver cooled to 4.2 K), again with a practical 10%–15% bandwidth [24]–[26]. The 3×3 micromachined array allows the use of a backing magnet behind the antennas without interfering with the radiation patterns (necessary for proper operation of the SIS detectors), and allows ample space for the extraction of nine IF signals with high IF bandwidths.

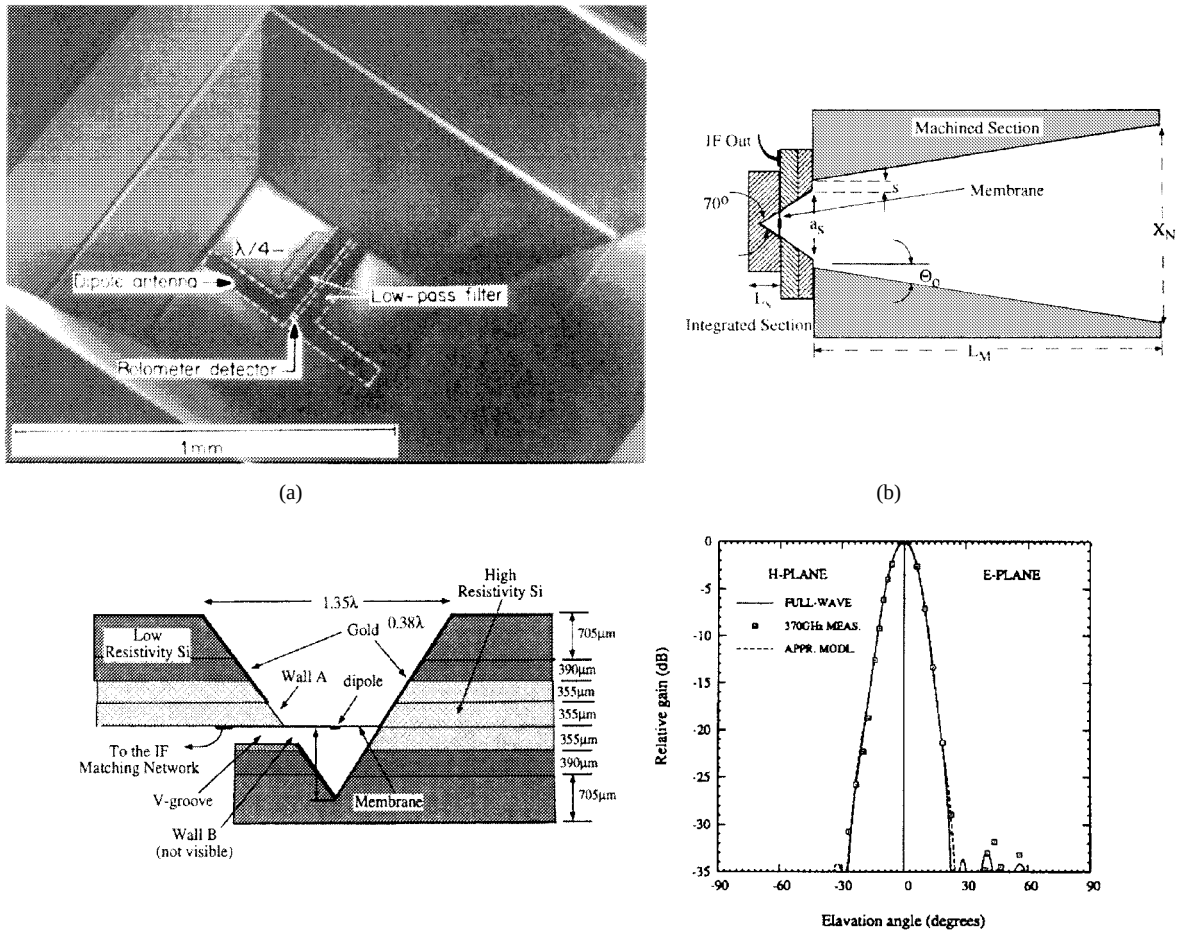

Fig. 7. (a) SEM photograph of a micromachined horn antenna. (b) Geometry of a 350-GHz integrated horn receiver with an extension section for improved Gaussian-coupling efficiency with $s = 0.085\lambda$, $a_s = 1.35\lambda$, $\theta_0 = 8.5°$, $L_M = 13\ \lambda$, $X_N = 54\lambda$. (c) Cross section of the antenna showing the location of the membrane (and the dipole/diode). (d) Measured patterns at 370 GHz with a comparison with theory. The Gaussian coupling efficiency is 97% [20].

B. Other Membrane-Type Antenna, Bolometer, SIS Detector, and Transmission-Line Structures

The membrane-type approach has also been applied to other antenna designs. A 100–800-GHz log-periodic antenna was integrated on a membrane and backed by an absorbing cavity [27]. A micromachined corner cube with a traveling-wave antenna on a membrane was developed for 2.5-THz applications and resulted in 18–19-dB gain [28]. This type of antenna is particularly well suited for Schottky-diode detectors since the feed of the traveling-wave antenna is at the silicon (or GaAs)–membrane interface. A double-dipole antenna integrated on a membrane and backed by a ground plane was used as a feed for a small parabolic reflector (5-mm diameter) and resulted in a directivity of 37 dB at 2.5 THz [29]. This antenna is well suited for SIS detectors or hot-electron bolometers at 800 GHz and above. Also, a broken linearly tapered slot antenna (BLTSA) on a thin dielectric membrane was developed for use at 350 and 802 GHz, and resulted in symmetrical patterns with a 10-dB beamwidth of 44° [30]. The BLTSA has been used at 500 GHz with a hot-electron bolometer detector and provided good radiation patterns and receiver performance [31].

Another application of dielectric membranes is in bolometric detectors. The membrane provides heat isolation from the substrate and, therefore, results in bolometers with high responsivity and low-noise equivalent power (NEP) [32], [33]. A large area bismuth bolometer was developed on a membrane as a power-density sensor for terahertz frequencies, and operated successfully from 100 to 10 THz. The 1-μm membrane is electrically thin even at 10 THz and, therefore, does not affect the bolometer bandwidth. The bolometer performance was limited by $1/f$ noise, and a minimum power density of around 100 nW/cm^2 could be detected. Still, easy calibration of absolute power at terahertz frequencies was possible. Bolometric-type detectors have also been used with integrated horn antennas and have achieved a record room-temperature NEP of 8.3×10^{-11} W/Hz$^{1/2}$ measured at 1-kHz chopping frequency [34].

A thin membrane "window" has also been recently demonstrated inside an 850-GHz SIS waveguide receiver. In a typical configuration, an SIS detector is integrated on a thin quartz wafer. However, the required thickness of the wafer and the dimensions of the channel that hold the junction become too small at high frequencies for practical fabrication and assembly. In this application, the SIS device was integrated on a l-μm membrane, which, while electrically thin, could provide adequate support from the surrounding silicon wafer. The resulting receiver showed an uncorrected receiver noise

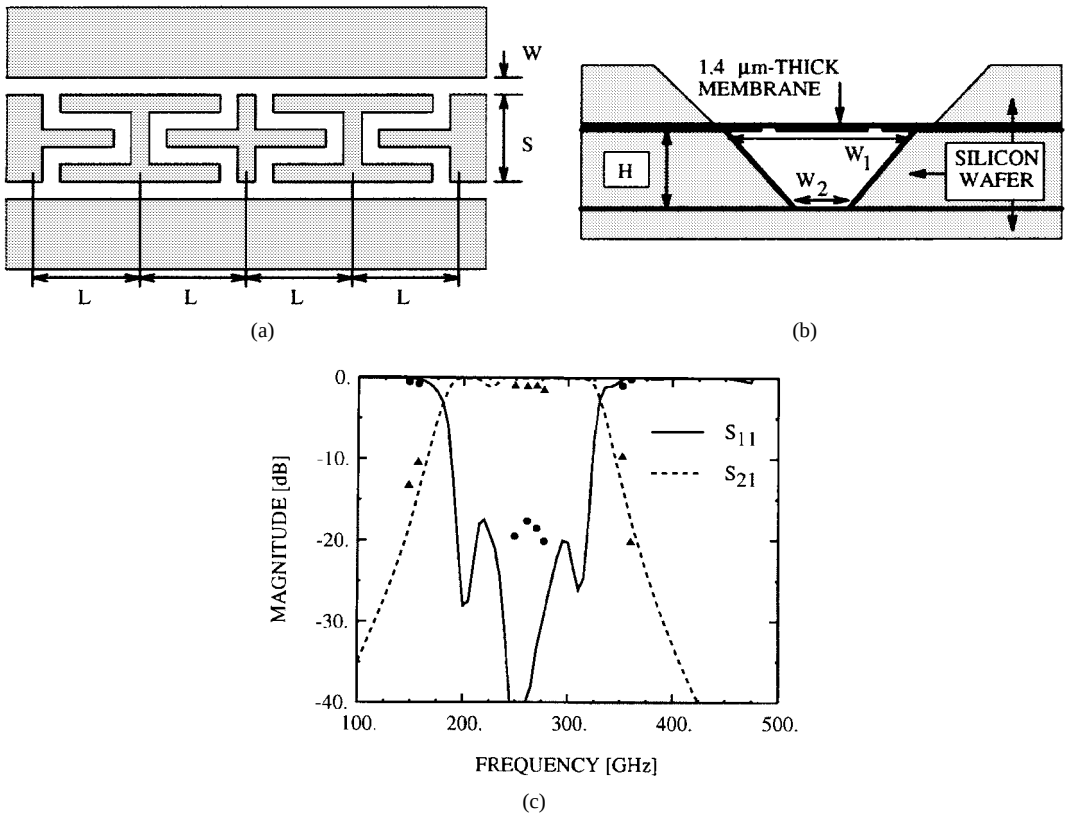

Fig. 8. (a) Metallization pattern for the four-section microshield bandpass filter (not to scale). (b) Cross-sectional view. (c) Comparison between measured and simulated results at 150–350 GHz [37]. Dimensions are: $L = 250\,\mu$m, $S = 50\,\mu$m, $W = 10\,\mu$m, $H = 200\,\mu$m, $W_1 = 320\,\mu$m, and $W_2 = 40\,\mu$m.

temperature of 514 K at 800–840 GHz when the mixer was cooled to 4.2 K [35].

Dielectric membranes have also been used to support terahertz transmission lines and filters. The loss for a membrane-supported coplanar-strip transmission line (CPS) (20-μm strip width, and 20-μm separation) was measured from 100 GHz to 1 THz using electrooptic techniques, and was less than 0.1 Np/mm at 1 THz, compared to 1.5 Np/mm for the same line on GaAs [36]. One very practical micromachined transmission-line topology is a type of shielded coplanar waveguide (CPW) called the microshield line. The microshield line was utilized to fabricate the first planar bandpass filter at 250 GHz [37]. The bandpass filter has a relative bandwidth of 58% and utilizes four quarter-wavelength open-end series stubs, as shown in Fig. 8(a). The filter is 1-mm-long, which is around $0.8\lambda_g$, at 250 GHz, where λ_g is the effective guided wavelength for the transmission line. The microshield filter is contained in a cavity, with dimensions given in Fig. 7(b), and the dominant waveguide-mode cutoff frequency for this structure is greater than 500 GHz. The measured results for this filter in Fig. 8(c) show a 1.0–1.5-dB passband insertion loss and excellent stopband rejection. This, and the preceding examples, demonstrate the significant performance benefits available through the simple micromachining of membrane structures.

IV. Micromechanically Adjustable Components

Micromachining techniques have also been used to provide integrated adjustable components which add the benefit of post-fabrication tuning and performance optimization to terahertz circuits. These *moving* components provide conventional mechanical circuit adjustments, yet have structures which are uniquely suited to photolithographic fabrication, planar circuitry, and micromanipulation.

The first (and only) micromechanically adjustable component demonstrated at submillimeter frequencies is the sliding planar backshort (SPB). It was developed to provide continuously adjustable tuning, like that of waveguide backshorts, to terahertz integrated circuits. An SPB tuner, illustrated in Fig. 9(a), consists of a movable patterned metal plate, which is fabricated as an integrated part of a coplanar transmission line. The pattern is designed to form a selective broad-band RF short circuit on the transmission line beneath it, and can be arbitrarily positioned along the line to vary the electrical length. The reflection coefficient S_{11} was measured at -0.02 dB for a 2-GHz CPW model and -0.3 dB for a 2-GHz CPS model, which was consistent with circuit measurements at 620 [38] and 100 GHz [39], respectively.

The entire micromechanical SPB tuning structure is fabricated through micromachining techniques developed to be compatible with those commonly in terahertz integrated circuits [40]. The procedure for fabricating a 620-GHz SPB is illustrated in Fig. 9(b). A coplanar transmission line is first (sputter) coated with a thin dielectric layer (SiO_2), and then covered with a sacrificial patch of thin-film metal (Cu), deposited and photo patterned over the region where the SPB will be positioned. A thick 8-μm layer of photoresist is deposited over this metal, and patterned to allow the 5-μm-thick SPB plate structure to be formed through electroplating

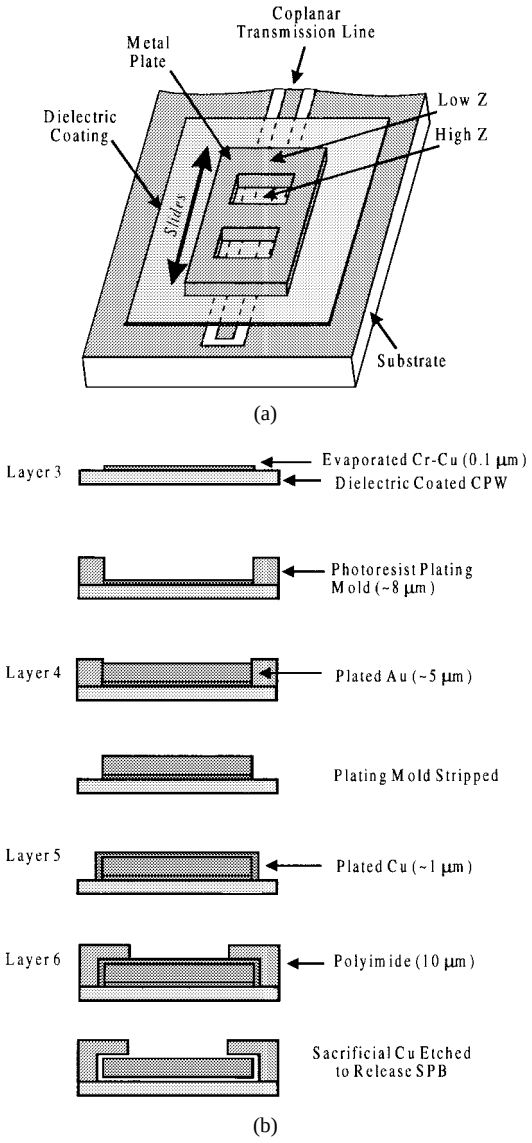

Fig. 9. (a) Concept and (b) fabrication overview for an integrated SPB demonstrated at 620 GHz. Micromachining techniques made compatible with terahertz integrated-circuit technology are used to form a guide-restricted metal pattern (200-μm-wide, 5-μm-thick) which slides over a dielectric-coated coplanar transmission line to vary the electrical length [40].

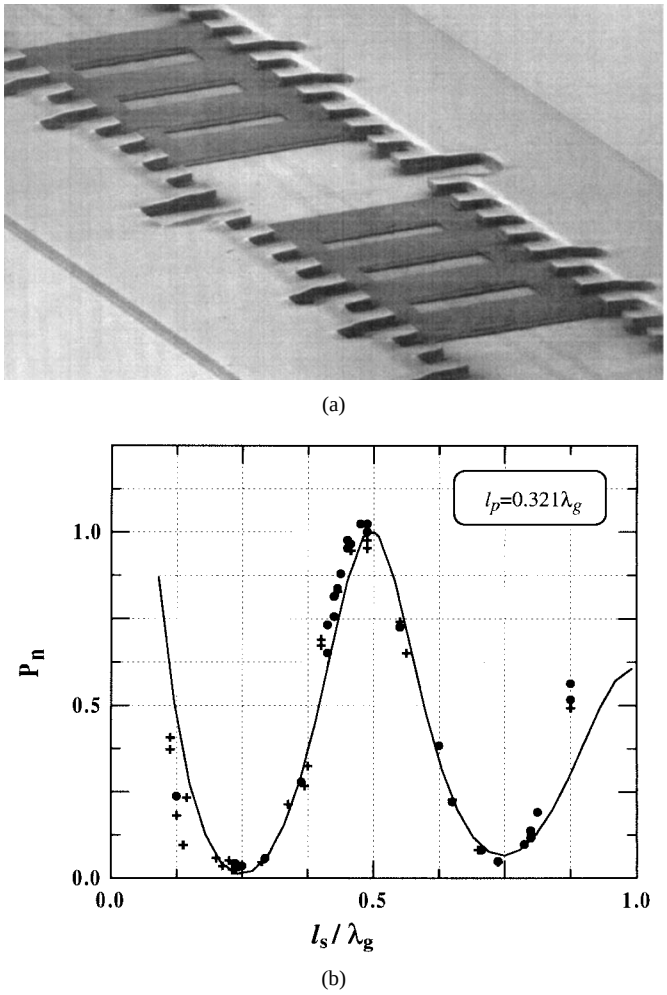

Fig. 10. (a) SEM photograph. (b) Measured performance for a quasi-optical 620-GHz monolithic detection circuit with two integrated SPB tuners. The two tuners consist of five high/low impedance sections (each 70–80-μm-long), and are integrated with CPW transmission lines (16-μm-wide center conductor, 8-μm gaps), as series and parallel tuners used to vary the power delivered from a slot antenna to a bismuth detector over a range of nearly 15 dB. The normalized detected power P_n is shown as a function of the series tuning element position I_s for a fixed position of the parallel tuning element [38].

(Au). The resist is stripped, and the entire metal structure is electroplated with about 1 μm of sacrificial metal (Cu). A thick 10-μm layer of polyimide is deposited and photo patterned to form strips which anchor to the substrate, and partially overlap the edges of the two sides of the metal structure. Finally, all of the sacrificial metal is etched away, releasing the SPB plate to move freely along the length of the line, within the confines of the polyimide guide strips. The SPB plate structure is 200-μm-wide, about 5-μm-thick, and consists of five or more covered/uncovered sections, each roughly $\lambda_g/4$ long. On an SiO_2 substrate ($\lambda_g = 312\,\mu$m), covered sections are 80-μm-long, and uncovered sections are 65- and 75-μm-long.

The performance of two mechanically manipulated SPB tuners has been successfully demonstrated in a 620-GHz quasi-optical monolithic integrated circuit, varying the power delivered from a planar antenna to a thin-film thermal detector over a range of nearly 15 dB. The circuit used a dielectric-filled parabola [41] to focus radiation onto a slot antenna, and coupled this radiation to a bismuth detector by means of two CPW transmission lines (with 8-μm gaps and a 16-μm-wide center conductor), each with integrated SPB tuners. One SPB was used to create a variable series reactance between the antenna and detector, potentially serving to compensate for any off-resonance reactance of the slot. The other SPB created a variable susceptance in parallel with the detector, and could act to compensate for the parasitic capacitance found in some common submillimeter-wave devices. An SEM photograph of the circuit is shown in Fig. 10(a), and the normalized power delivered to the detector P_n is shown in Fig. 10(b) as a function of the position of the series tuning element l_s for a fixed position of the parallel tuning element.

This versatile sliding structure can be readily implemented in a wide range of terahertz integrated circuits to serve as transmission-line tuners, antenna elements, shutters, and other adjustable components. The monolithic design of the

SPB makes it suitable for scaling to several terahertz, where the aspect ratio of the tuner is actually more suitable for conventional photolithographic thin-film techniques. However, the smaller structure and shorter wavelength would make it more difficult to manipulate the tuner externally and, thus, some form of integral electromechanical actuation would be desirable. Electrostatic techniques [42] and thin-film shape-memory alloys [43] offer promise for this function.

V. Conclusion

This paper summarizes recent micromachining research efforts for terahertz applications. A large part of this paper has been directed at the development of antennas and front-end components, which can be integrated in large numbers for focal-plane arrays or low-cost terahertz systems. Waveguide antennas, transmission lines, and mixer block assemblies have been fabricated through various economical micromachining techniques, with performance comparable to that of costly conventionally produced components. Practical techniques have also been developed to improve the performance of terahertz integrated circuits, through substrate removal and the integration of adjustable micromechanical tuning elements. These approaches offer great potential for the production of intricate terahertz systems, which can serve to advance the state-of-the-art in space and atmospheric research, and to extend the use of the terahertz spectrum to broader industrial and commercial applications.

References

[1] J. W. Waters, "Submillimeter-wavelength heterodyne spectroscopy and remote sensing of the upper atmosphere," *Proc. IEEE*, vol. 80, pp. 1679–1701, Nov. 1992.

[2] T. G. Phillips and J. Kreene, "Submillimeter astronomy," *Proc. IEEE*, vol. 80, pp. 1662–1678, Nov. 1992.

[3] P. F. Goldsmith, C.-T. Hsieh, G. R. Huguenin, J. Kapitzky, and E. L. Moore, "Focal plane imaging systems for millimeter wavelengths," *IEEE Trans. Microwave Theory Tech.*, vol. 41, pp. 1664–1675, Oct. 1993.

[4] D. B. Rutledge, S. E. Schwarz, T. L. Hwang, D. J. Angelakos, K. K. Mei, and S. Yokota, "Antennas and waveguides for far-infrared integrated circuits," *IEEE J. Quantum Electron.*, vol. QE-16, pp. 508–516, May 1980.

[5] W. R. McGrath, C. K. Walker, M. Yap, and Y.-C. Tai, "Silicon micromachined waveguides for millimeter-wave and submillimeter-wave frequencies," *IEEE Microwave Guided Wave Lett.*, vol. 3, pp. 61–63, Jan. 1993.

[6] J. A. Wright, S. Tatic-Lucic, Y.-C. Tai, W. R. McGrath, B. Bumble, and H. LeDuc, "Integrated silicon micromachined waveguide circuits for submillimeter wave applications," in *6th Int. Symp. Space Terahertz Technol.*, Pasadena, CA, Mar. 1995, pp. 387–396.

[7] K. E. Peterson, "Silicon as a mechanical material," *Proc. IEEE*, vol. 70, pp. 420–457, May 1982.

[8] J. W. Digby *et al.*, "Integrated micromachined antenna for 200 GHz operation," in *IEEE MTT-S Int. Microwave Symp. Dig.*, Denver, CO, June 1997, pp. 561–564.

[9] C. M. Mann, J. L. Hesler, P. J. Koh, T. W. Crowe, W. L. Bishop, R. M. Weikle, and D. N. Matheson, "A versatile micromachined horn antenna," in *20th ESTEC Antenna Workshop Millimeter Wave Antenna Technol. Antenna Measurements*, Noordwig, The Netherlands, June 1997.

[10] T. W. Crowe *et al.*, "Inexpensive receiver components for millimeter wavelengths," in *8th Int. Symp. Space Terahertz Technol.*, Cambridge, MA, Mar. 1997, pp. 377–384.

[11] S. T. G. Wootton, S. R. Davies, and N. J. Cronin, "A novel micromachined 1.6 THz mixer," in *22nd Int. Conf. Infrared Millimeter Waves*, Cambridge, MA, July 1997, pp. 132–133.

[12] K. Y. Lee *et al.*, "Micromachining applications of a high resolution ultrathick photoresist," *J. Vac. Sci. Technol. B, Microelectron. Process. Phenom.*, vol. 13, no. 6, pp. 3012–3016, Nov.–Dec. 1995.

[13] V. M. Lubecke, C. M. Mann, and K. Mizuno, "Practical micromachining techniques for high aspect ratio submillimeter wave components," in *9th Int. Symp. Space Terahertz Technol.*, Pasadena, CA, Mar. 1998.

[14] V. M. Lubecke, T. Hamano, C. M. Mann, and K. Mizuno, "Micromachining of photo-plastic submillimeter wave components," in *Proc. Asia–Pacific Microwave Conf.*, Yokohama, Japan, Dec. 1998.

[15] C. K. Walker *et al.*, "Laser micromachining of silicon: A new technique for fabricating high quality terahertz waveguide components," in *8th Int. Symp. Space Terahertz Technol.*, Cambridge, MA, Mar. 1997, pp. 358–376.

[16] T. Crowe, private communication, Feb. 1998.

[17] D. B. Rutledge, S. E. Schwarz, and A. T. Adams, "Infrared and submillimeter antennas," *Infrared Phys.*, vol. 18, pp. 713–729, 1978.

[18] G. M. Rebeiz, D. P. Kasilingam, Y. Guo, P. A. Stimpson, and D. B. Rutledge, "Monolithic millimeter-wave two-dimensional horn imaging arrays," *IEEE Trans. Antennas Propagat.*, vol. 38, pp. 1473–1482, Sept. 1990.

[19] W. Y. Ali-Ahmad, G. M. Rebeiz, G. Chin, and H. Davee, "802 GHz integrated horn antennas imaging array," *Int. J. Infrared Millimeter Waves*, vol. 12, pp. 481–486, May 1991.

[20] G. V. Eleftheriades and G. M. Rebeiz, "Analysis and design of millimeter-wave quasi-integrated horn antennas," *IEEE Trans. Microwave Theory Tech.*, vol. 41, pp. 54–965, June–July 1993.

[21] W. Y. Ali-Ahmad and G. M. Rebeiz, "An 86–106 GHz quasi-integrated low-noise receiver," *IEEE Trans. Microwave Theory Tech.*, vol. 41, pp. 558–564, Apr. 1993.

[22] W. Y. Ali-Ahmad, W. L. Bishop, T. W. Crowe, and G. M. Rebeiz, "250 GHz quasi-integrated low-noise Schottky-receiver," *Int. J. Infrared Millimeter Waves*, vol. 14, pp. 737–748, Apr. 1993.

[23] W. Y. Ali-Ahmad and G. M. Rebeiz, "A 335 GHz integrated Schottky receiver," *IEEE Microwave Guided Wave Lett.*, vol. 4, pp. 37–39, Feb. 1994.

[24] E. Garcia, B. R. Jacobson, and Q. Hu, "Fabrication of high-quality SIS junctions on thin SiN membranes," *Appl. Phys. Lett.*, vol. 63, p. 1002, 1993.

[25] G. de Lange, B. R. Jacobson, and Q. Hu, "A low-noise micromachined millimeter-wave heterodyne mixer with Nb superconducting tunnel junctions," *Appl. Phys. Lett.*, vol. 68, p. 1862, 1996.

[26] G. de Lange, A. Rahman, E. Duerr, and Q. Hu, "Low-noise micromachined SIS mixers for millimeter-wave imaging arrays," *IEEE Trans. Appl. Superconduct.*, vol. 7, pp. 3593–3596, June 1997.

[27] G. M. Rebeiz, W. Regehr, D. B. Rutledge, R. L. Savage, and N. C. Luhmann, Jr., "Submillimeter-wave antennas on thin membranes," *Int. J. Infrared Millimeter Waves*, vol. 8, pp. 1249–1256, Oct. 1987.

[28] S. S. Gearhart, C. C. Ling, G. M. Rebeiz, H. Davee, and G. Chin, "Integrated 119-μm linear corner-cube array," *IEEE Microwave Guided Wave Lett.*, vol. 1, pp. 155-157, July 1991.

[29] D. F. Filipovic, W. A. Ali-Ahmad, and G. M. Rebeiz, "Millimeter-wave double-dipole antennas for high-gain integrated reflector illumination," *IEEE Trans. Microwave Theory Tech.*, vol. 40, pp. 962–967, May 1992.

[30] P. R. Acharya, H. Ekstrom, S. S. Gearhart, J. F. Johansson, S. Jacobson, G. M. Rebeiz, and E. L. Kollberg, "Tapered slotline antennas at 802 GHz," *IEEE Trans. Microwave Theory Tech.*, vol. 41, pp. 1715–1719, Oct. 1993.

[31] Y. P. Goussev *et al.*, "Quasioptical superconducting hot electron bolometer for submillimeter-waves," *J. Infrared Millimeter-Waves*, vol. 17, no. 2, pp. 317–331, 1996.

[32] C. C. Ling and G. M. Rebeiz, "A wide-band monolithic quasi-optical power meter for millimeter-wave and submillimeter-wave applications," *IEEE Trans. Microwave Theory Tech*, vol. 39, pp. 1257–1261, Aug. 1991.

[33] C. C. Ling, J. C. Landry, H. Davee, G. Chin, and G. M. Rebeiz, "Large area bolometers for THz power measurements," *IEEE Trans. Microwave Theory Tech.*, vol. 42, pp. 758–760, Apr. 1994.

[34] A. Rahman, G. de Lange, and Q. Hu, "Micromachined room-temperature microbolometers for millimeter-wave detection," *Appl. Phys. Lett.*, vol. 68, p. 2020, 1996.

[35] J. W. Kooi, J. Pety, B. Bumble, C. K. Walker, H. G. LeDuc, P. L. Schaffer, and T. G. Phillips, "An 850 GHz waveguide receiver employing a niobium SIS junction fabricated on a 1-μm Si_3N_4 membrane," *IEEE Trans. Microwave Theory Tech.*, vol. 46, pp. 151–161, Feb. 1998.

[36] H. J. Cheng, J. F. Whitakker, T. M. Weller, and L. P. Katehi, "Terahertz-bandwidth characteristics of coplanar transmission-lines on low permittivity substrates," *IEEE Trans. Microwave Theory Tech.*, vol. 42, pp. 2399–2406, Dec. 1994.

[37] T. M. Weller, L. P. Katehi, and G. M. Rebeiz, "A 250-GHz microshield bandpass filter," *IEEE Microwave Guided Wave Lett.*, vol. 5, pp. 153–155, May 1995.
[38] V. M. Lubecke, W. R. McGrath, P. A. Stimson, and D. B. Rutledge, "Micromechanical tuning elements in a 620 GHz integrated circuit," *IEEE Trans. Microwave Theory Tech.*, to be published.
[39] V. M. Lubecke, W. R. McGrath, and D. B. Rutledge, "A 100-GHz coplanar strip circuit tuned with a sliding planar backshort," *IEEE Microwave Guided Wave Lett.*, vol. 3, pp. 441–443, Dec. 1993.
[40] V. M. Lubecke, W. R. McGrath, Y.-C. Tai, and D. B. Rutledge, "Microfabrication of linear translator tuning elements in submillimeter wave integrated circuits," *IEEE J. Microelectromech. Syst.*, to be published.
[41] P. H. Siegel and R. J. Dengler, "The dielectric-filled parabola: A new millimeter and submillimeter wavelength receiver/transmitter front end," *IEEE Trans. Antennas Propagat.*, vol. 39, pp. 40–47, Jan. 1991.
[42] T. Akiyama and K. Shono, "Controlled stepwise motion in polysilicon microstructures," *IEEE J. Microelectromech. Syst.*, vol. 2, pp. 106–110, Sept. 1993.
[43] P. Krulevitch, A. P. Lee, P. B. Ramsey, J. C. Trevino, J. Hamilton, and M. A. Northrup, "Thin film shape memory alloy microactuators," *IEEE J. Microelectromech. Syst.*, vol. 5, pp. 270–282, Dec. 1996.

Victor M. Lubecke (S'86–M'86–A'95) received the B.S. degree in electrical and electronic engineering from the California State Polytechnical University, Pomona, in 1986, and the M.S. and Ph.D. degrees in electrical engineering form the California Institute of Technology, Pasadena, CA, in 1990 and 1995, respectively.

From 1987 to 1996, he worked at the NASA Jet Propulsion Laboratory, Pasadena, CA, where he was involved with millimeter and submillimeter-wave technology in space communications and remote sensing applications. Since 1996, he has been a Visiting Researcher at the Photodynamics Research Center, Institute for Physical and Chemical Research (RIKEN), Sendai, Japan. His current research interests include high-frequency integrated circuits, quasi-optics, and related MEMS techniques.

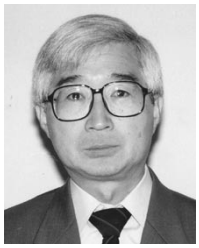

Koji Mizuno (M'72–SM'72–F'93) was born in Sapporo, Hokkaido, Japan, on July 17, 1940. He received the B. Eng., M. Eng., and D. Eng. degrees in electronic engineering from Tohoku University, Sendai, Japan, in 1963, 1965, and 1968, respectively.

In 1968, he joined the Department of Electronic Engineering, Faculty of Engineering, Tohoku University, was appointed Associate Professor at Research Institute of Electrical Communication, in 1972, and since 1984, has been a Professor of electron devices. In 1973, he spent a one-year sabbatical leave at Queen Mary College, University of London, U.K., and in 1990, spent a six-month sabbatical leave at the California Institute of Technology, Pasadena, and Queen Mary and Westfield College, London, U.K. From 1990 to 1998, he was a Team Leader of the Photodynamics Research Center, Institute of Physical and Chemical Research (RIKEN), Sendai, Japan, where he ran a laboratory for submillimeter-wave research, as well as a laboratory at Tohoku University. He has been interested in the millimeter and submillimeter-wave region of the electromagnetic-wave spectrum, and his current work is in detection, generation and their applications in the region.

Dr. Mizuno is a member of the Institute of Electronics, Information and Communication Engineers, (IEICE), Japan, the Institute of Electrical Engineers of Japan, and the Japan Society of Applied Physics. He was awarded the 17th Kagaku-Keisoku-Shinko-Kai (Scientific Measurement) Award in 1984 and the Kenneth J. Button Prize in 1998 for developments of millimeter and submillimeter-wave devices.

Gabriel M. Rebeiz (S'86–M'88–SM'93–F'97) received the Ph.D. degree in electrical engineering from the California Institute of Technology, Pasadena, in 1988.

In September 1988, he joined the faculty of the University of Michigan at Ann Arbor, and was promoted to Full Professor in May 1998. He has held short visiting professorships at Chalmers University of Technology, Gothenburg, Sweden, Ecole Normale Superieur, Paris, France, and Tohoku University, Sendai, Japan. His research interest includes applying micromachining techniques and MEMS for the development of novel components and subsystems for wireless communication systems. He is also interested in Si/GaAs RFIC design for receiver applications, and in the development of planar antennas and microwave/millimeter-wave front-end electronics for applications in millimeter-wave communication systems, automotive collision-avoidance sensors, monopulse tracking systems, and phased arrays.

Prof. Rebeiz was the recipient of the National Science Foundation Presidential Young Investigator Award in 1991 and the URSI International Isaac Koga Gold Medal Award for Outstanding International Research in 1993. He also received the Research Excellence Award in 1995 from the University of Michigan at Ann Arbor. Together with his students, he was the winner of Best Student Paper Awards presented by the IEEE Microwave Theory and Techniques Society (1992, 1994–1998), and the IEEE Antennas and Propagation Society (1992, 1995), and received the JINA'90 Best Paper Award. He also received the University of Michigan at Ann Arbor EECS Department Teaching Award in October 1997, and was selected by the students as the 1997–1998 Eta Kappa Nu EECS Professor of the Year. In June 1998, he received the Amoco Foundation Teaching Award, which is presented annually to one (or two) faculty members at the University of Michigan at Ann Arbor, for excellence in undergraduate teaching.